

Unsupervised Data Selection for Data-Centric Semi-Supervised Learning

Xudong Wang*
UC Berkeley/ICSI

xdwang@eecs.berkeley.edu

Long Lian*
UC Berkeley/ICSI

longlian@berkeley.edu

Stella X. Yu
UC Berkeley/ICSI

stellayu@berkeley.edu

Abstract

We study unsupervised data selection for semi-supervised learning (SSL), where a large-scale unlabeled dataset is available and a small subset of data is budgeted for label acquisition. Existing SSL methods focus on learning a model that effectively integrates information from given small labeled data and large unlabeled data, whereas we focus on selecting the right data to annotate for SSL without requiring any label or task information. Intuitively, instances to be labeled shall collectively have maximum diversity and coverage for downstream tasks, and individually have maximum information propagation utility for SSL. We formalize these concepts in a three-step data-centric SSL method that improves FixMatch in stability and accuracy by 8% on CIFAR-10 (0.08% labeled) and 14% on ImageNet-1K (0.2% labeled). It is also a universal framework that works with various SSL methods, delivering consistent performance gains. Our work demonstrates that small computation spent on carefully selecting data for annotation brings big annotation efficiency and model performance gain without changing the learning pipeline. Our completely unsupervised data selection can be easily extended to other weakly supervised learning settings.

1. Introduction

Deep learning (DL) has achieved tremendous success on various tasks including natural language understanding [17], visual object recognition [40] and object detection [27], following a straightforward recipe: refining model architectures, learning from large amounts of data, and scaling computation [28, 35, 41, 68]. It is observed that their success is partially attributable to their scalability, but the performance advantages conferred by a larger dataset can come at a considerable cost, which can be extreme when data labeling is challenging or expensive [3, 59].

With a limited labeling budget, semi-supervised learning (SSL) methods boost performance by learning from a

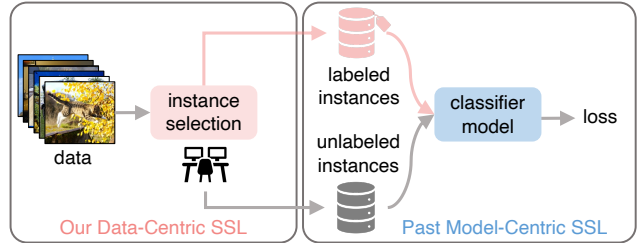


Figure 1. We consider the novel task of unsupervised data selection for semi-supervised learning (SSL). Existing SSL methods focus on training the best model given labeled and unlabeled data, whereas we focus on selecting labeled data for annotation.

small set of labeled data and large-scale unlabeled data. In SSL, while labeled data provides direct supervision on the classifier, unlabeled data helps regularize the classifier in terms of smoothness and sharpness, captured by consistent [3, 4, 42, 54, 59, 61, 67] and minimal entropy [4, 29, 42] predictions respectively. Recent development of SSL methods only require a very small number of labeled samples to achieve accuracy comparable to supervised training. With only 13 labeled images per class on ImageNet, [12] achieves 76.6% Top-1 accuracy. In such a low-shot setting, the quality of the labeled dataset is of paramount importance. For example, if we fix the selection of labeled samples, the standard deviation among 5 runs drop from 3.18% to 0.4% on CIFAR-10 with 40 labeled samples using SimCLRv2-CLD [12, 63]. While a well-chosen labeled image is representative of a large group of similar images in the test set, an outlier could disturb the decision boundary and even result in model collapsing in training.

However, for researchers and developers on SSL and many other areas, how to obtain labeled samples is often the less incentivized aspect, whereas building novel models and algorithms is often regarded as the lionized work.

Most previous SSL methods adopt random sampling or stratified sampling by category [3, 59] as the instance sampling strategy for studying SSL on fully-labeled datasets. Each sampler has its own caveats: Random sampling can fail to cover all semantic categories and lead to poorer performance and model instability, whereas stratified sampling

*equal contribution

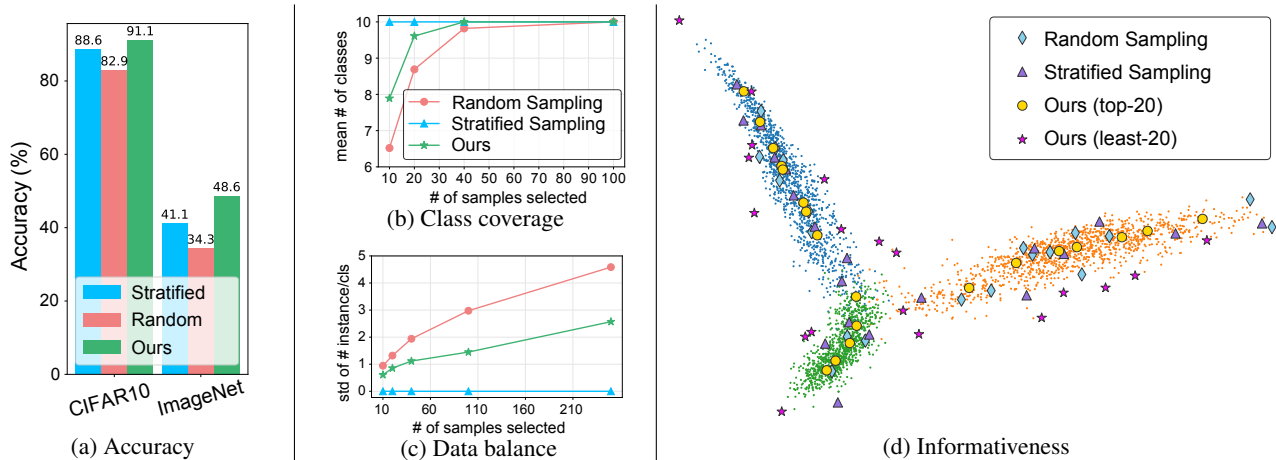


Figure 2. By selecting representative and diversified samples, we achieve significant improvements to other sampling methods. (a) shows rises in downstream classification accuracy on FixMatch; (b) shows DC-SSL covers all semantic classes with only few samples; (c) shows DC-SSL’s selection is much more balanced than random sampling baseline; (d) visualizes selections from a toy dataset (3 classes in ImageNet). Ours (top-20/least-20) indicates the 20 instances with highest/lowest metric value, respectively. Our selections (i.e. instances with highest metric value) consistently cover informative samples across the space, while instances with lowest metric value are almost always outliers. (best viewed in color and zoomed in)

is often unrealistic, especially when the number of classes is large: If we can sample data by their categories, we would already have the label of every instance!

In contrast to previous SSL methods, which mostly focus on improving the model architecture and optimization, our data-centric SSL addresses an *unsupervised data selection* problem (Fig. 1): Given an SSL model, among many possible ways to select a small fixed number of instances in the sea of unlabeled data for labeling, which way would lead to the best SSL model performance, given no labels and thus no idea what the downstream classification task would be? This task is also in a stark contrast to supervised data selection for active learning (AL), which is conditioned on an initial labeled set and for the benefit of the particular supervised classification task.

We develop a **Data-Centric SSL (DC-SSL)** approach based on the intuition that ideal instances to be labeled shall collectively have maximum diversity and coverage for downstream classification tasks, and individually have maximum information propagation utility for SSL. It has three steps:

1. Unsupervised feature learning that maps data into a maximally discriminative feature space.
2. Select top- m representative instances for labeling per diversity, coverage, and information utility.
3. Apply an SSL method, e.g. FixMatch, on the selected labeled data and the rest unlabeled data.

Our result analysis shows several benefits over past model-centric SSL methods (Fig. 2):

- **On classification accuracy (Fig. 2a):** Just by selecting the right data to label, we improve the classification accuracy of FixMatch by an astonishing 8% and 14% in CIFAR-10 (with 0.08% labeled) and ImageNet-1k (with

0.2% labeled). These results are even better than from the practically infeasible stratified sampling which assumes perfectly balanced labeled instances.

- **On class coverage (Fig. 2b) and data balance (Fig. 2c):** Our method covers more classes of CIFAR-10 with a much smaller labeling budget and a more balanced distribution over classes: Ours cover 9.5 out of 10 classes on average when only 20 samples are selected for labeling. The standard deviation on the number of samples per class is also greatly reduced, resulting in a more uniform distribution over classes.
- **On informativeness (Fig. 2d):** Our method successfully discovers most representative and diversified samples from the unlabeled data of ImageNet: The 20 selected instances tend to be located near density peaks; they are tightly connected to a large number of neighbors and spread out more uniformly in the feature space, allowing labeling information to propagate more effectively and widely. However, random and stratified sampling pick less informative outliers far too often, resulting in low learning efficiency and sometimes even learning collapse. These reasons underlie our better performance over stratified sampling, even though it is guaranteed to have balanced labeled data across classes. Note that our least-20 samples have the lowest utility values, lying in sparse areas with the weakest propagation abilities.

Our work shows that small computation spent on carefully selecting data for annotation brings big annotation efficiency and performance gain without changing the learning pipeline. Our completely unsupervised data selection can be easily extended to other weakly supervised learning settings.

2. Related Work

Semi-supervised Learning (SSL) integrates information from both small labeled data and large unlabeled data. **Consistency based regularization** [54,61,67] applies a consistency term to the final loss by imposing invariance on unlabeled data under augmentations. **Pseudo-labeling**, also known as self-training [3,4,42,59], relies on the model’s high confidence predictions to produce pseudo-labels of unlabeled data and trains them jointly with labeled data. FixMatch [59] integrates strong data augmentation [18], pseudo-labels filtering [44] and temperature re-scaling to achieve the current SOTA on SSL. It also explores training on the most representative samples ranked by [8]. However, [8] is a supervised method that requires the use of all data labels. As a two-stage method, SimCLRv2 [12] is a transfer learning method for SSL: It applies contrastive learning on unlabeled data, followed by supervised learning on labeled data. **Entropy-minimization** [4,29,42] assumes that classification boundaries do not pass through high-density area of marginal distributions, enforcing confident predictions on unlabeled data.

These SSL methods choose data to label by random sampling which leads to poor performance, or by stratified sampling that selects the same number of samples per category, assuming unrealistically that labels are available on all the data. Instead of focusing on novel models and algorithms, our method is *data-centric*, focusing on choosing the right samples for effective SSL.

Self-supervised Learning learns representations transferable to downstream tasks without annotations [30,65]. **Contrastive learning** [11,33,63,65] learns representations that map similar samples or different augmentations of the same instance close and dissimilar instances apart. **Similarity-based** methods [30] learn representations without negative pairs by predicting the embedding of a target network with an online network. **Feature learning with grouping** [9,10,63,66,70,73] respects the natural grouping of data by exploiting clusters in the latent representation. We study unlabeled data in a unsupervisedly learned feature space, due to its high quality and low feature dimensions.

Active Learning (AL) aims to select a small subset of labeled data to achieve competitive performance over supervised learning on fully labeled data [5,16,52]. **Conventional AL** has three major camps [51,56]: membership query synthesis [1], stream-based selective sampling [2,19], and pool-based active learning [36,62,64]. In **Deep AL**, Core-Set [55] approaches data selection as a set cover problem and with a derived upper bound it is equivalent to the k-Center problem. Adversarial-based approaches [22] use adversarial samples to estimate distance from decision boundaries based on sensitivity to adversarial attacks. Learning Loss for Active Learning [71] makes use of a novel parametric module to predict target losses of unlabeled data and queries the instance with largest loss for label.

Approaches	SSL	AL	SSAL	DC-SSL
Uses no initial random labels	✗*	✗	✗	✓
Actively queries for labels	✗	✓	✓	✓
Requires annotation only once	✓	✗	✗	✓
Leverages unlabeled data	✓	✗	✓	✓

Table 1. Comparisons of (MC-)SSL, AL, SSAL, and our proposed DC-SSL methods in key properties. Among them, we are the only approach that does not use any random labels in selection, which means much higher sample efficiency when compared to AL and SSAL approaches. *: except the ideal stratified sampling setting.

Semi-supervised Active Learning (SSAL) combines AL with SSL. [60] merges uncertainty-based metrics with MixMatch [4]. [26] merges consistency-based metrics with SSL. AL/SSAL often rely on initial labeled data to learn the model and sampler, requiring multiple (e.g. 10) rounds of sequential annotation and significant modifications on existing annotation pipelines. See more comparisons in Sec. 4.4.

A brief overview of the properties of SSL/AL/SSAL/DC-SSL is shown at Table 1. Our method has the advantage of active learning that seeks for the optimal samples to label, yet does not require initial random samples or multiple rounds of human intervention to finish annotation. Furthermore, our method leverages unlabeled data which is often cheap to acquire. When compared to SSAL, ours is much easier to implement because we do not require modifications on existing SSL training methods, while SSAL requires merging SSL and AL to a single stage. To our best knowledge, our work is the first *unsupervised* sampling method on large-scale recognition datasets that requests annotation only *once*, consistent with previous SSL pipelines.

3. Data-centric Semi-supervised Learning

Existing SSL methods are *model-centric*, focusing on novel models and algorithms. We instead explore *Data-Centric* Semi-Supervised Learning (DC-SSL), focusing on selecting the most informative data to label for effective SSL. DC-SSL has three steps: 1) Unsupervised feature learning; 2) Unsupervised sample selection for annotation; 3) Semi-supervised learning on selected labeled data and rest unlabeled data. In this section, we first define the problem and describe how our method solves it through selecting samples that are both representative and diverse.

3.1. Problem Setup

Consider a dataset $\mathbb{D} = (\mathbf{x}_i, y_i)_{i=1}^n$ with n images, and the labels y_i are not known unless we request annotation. Since there is no preview of y_i for *any* of the \mathbf{x}_i , stratified sampling that results in balanced labeled data per class is impossible, as commonly assumed in [3,12,59]. Given a limited labeling budget, our goal is to identify the top- m representative samples $\mathbb{A} = (\mathbf{x}_j, y_j)_{j=1}^m$ from \mathbb{D} to anno-

tate, so as to improve SSL performance jointly trained on unlabeled data \mathbb{D} and labeled data \mathbb{A} . Several popular SSL methods are utilized to verify the effectiveness of our data selection method while keeping the algorithms unchanged.

3.2. Unsupervised Representation Learning

We apply unsupervised feature learning to obtain a lower dimensional (128- D) representation that maximally maintains the individuality of each instance [11, 33, 48, 65]. During contrastive learning, we learn a mapping function f such that in the $f(x)$ feature space, instance x_i is attracted to its augmented version x'_i and repulsive to a different instance $x_j, j \neq i$. We model f by a convolutional neural network which maps x onto a d -dimensional hypersphere with L^2 normalization. To make a fair comparison with previous work [7, 59], we use MoCo v2 [13] to learn representations on ImageNet with instance-centric contrastive loss. The feature space representations of CIFAR-10 images are extracted with CLD [63], which adds an instance-group contrastive loss to improve feature quality. We refer readers to Appendix for formulations and interpretations of MoCo v2 and CLD.

3.3. Unsupervised Sample Selection for Annotation

We represent $(x_i)_{i=1}^n$ as a weighted graph $G = (V, E; W)$, where nodes are points in the feature space, and edges between nodes are attached with weights of pairwise feature similarity [6, 15, 20, 57]:

$$w_{ij} = \frac{1}{\|f(x_i) - f(x_j)\|} \quad (1)$$

where $f(x_i)$ is the L^2 normalized feature of V_i learned from e.g. MoCo v2 [13]. While w_{ij} is a bijection to cosine similarity $w_{ij} = \cos(V_i, V_j)$ in theory, we find that $1/\|f(x_i) - f(x_j)\|$ works better empirically than $\cos(V_i, V_j)$. See Appendix for more explanations.

Given a labeling budget of m instances, we aim to select m instances that are both *representative* to carry information to other examples and *diversified* for broad coverage. We evaluate the utility of each instance in terms of information transport efficiency on a graph.

Density estimation with K -NN. The most straightforward idea of sample selection for labeling is to select the well-connected node, which is most likely to spread semantic information to nearby nodes with the smallest cost. It corresponds to a density peak in the feature space. The basic K -nearest neighbour density (K -NN) estimate is constructed as follows [23, 46, 49]:

$$\hat{f}_{\text{KNN}}(V_i, K) = \frac{1}{n} \sum_{j=1}^K \frac{1}{A_d \cdot R_k^d(V_i)} \quad (2)$$

where $A_d = \frac{\pi^{d/2}}{\Gamma(\frac{d}{2}+1)}$ is the volume of a unit d -dimensional ball, $\Gamma(x)$ the Gamma function, $R_k^d(V_i)$ the distance between V_i and its K th nearest neighbor.

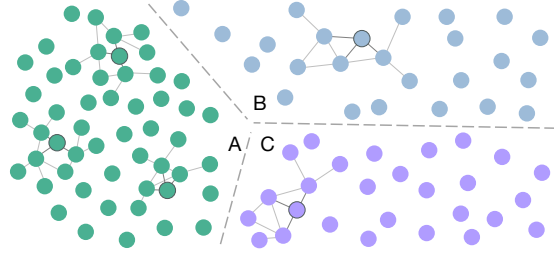


Figure 3. A case where local density alone gives bad querying results. If we only sample three instances to be annotated from the region with the highest estimated local density, only the three samples in cluster A will be queried due to their highest density. However, this may impair the ability of queries to capture multiple data distribution patterns and is less efficient in propagating semantic information to all unlabeled data.

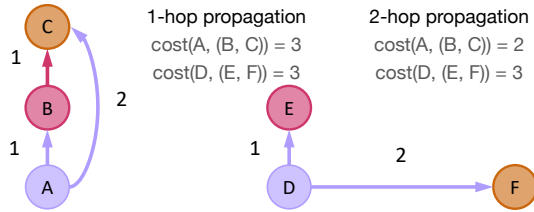


Figure 4. Two-hop propagation considers the indirect connection between two vertices and more accurately estimates the information dissemination ability of each vertex. The overall distance, i.e., $\text{cost}(\cdot)$, of propagating semantic information from vertex A to vertices B, C and vertex D to vertices E, F are illustrated, where the purple and magenta lines denote one-hop and two-hop propagation, respectively. Numbers in the figure are distances between two vertices.

Drawbacks of vanilla K -NN density estimation on self-supervised models. Despite its simplicity, directly selecting top samples according to vanilla k -NN density estimation has several drawbacks in our use cases: **1)** Only the K th nearest neighbor is referenced, while the relationships with all other $K-1$ points in the ball are not taken into consideration, rendering it sensitive to outliers. **2)** The densest peaks capture representativeness in local small regions but ignores global diversity (Fig. 3), which leads to redundancy along with insufficient coverage. **3)** Evaluating the utility of a node based on its direct neighbours ignores indirect connections between nodes (Fig. 4). It is likely to miss vertices (false negatives) without direct connections with anchored vertices, even if such vertices are well connected to anchored vertices through other intermediate vertices. **4)** Our unsupervisedly learned feature does not model semantics explicitly. In the following part of this section, we illustrate how our method solves the aforementioned issues.

Averaged distance function for robust density estimation. In contrast to the basic K -NN estimator, which uses the distance to the k th nearest neighbor alone for density

estimation, we consider all k neighbors instead:

$$\hat{f}_{\text{KNN}}(V_i, k) = \frac{k}{n} \frac{1}{A_d \cdot \frac{1}{k} \sum_{j=1}^k \frac{1}{w_{ij}}} \quad (3)$$

This improves our sensitivity to outliers and enables us to use larger k without losing focus on near neighbors, effectively enlarging our field of reception. We compare it to alternative formulations and show its advantage in Sec. 4.5. **Multi-hop propagation for measuring indirect connections between vertices.** To model indirect connections, we formulate the utility of vertex V_i with two-hop propagation:

$$U(V_i) = \hat{f}_{\text{KNN}}(V_i, K) + \sum_{\hat{V}_j \in B_{ik}} \cos(V_i, \hat{V}_j) \hat{f}_{\text{KNN}}(\hat{V}_j, K) \quad (4)$$

where $B_{ik} = \{\hat{V}_j' : \|V_i - \hat{V}_j'\| \leq R_k^d(V_i)\}$. Compared with one-hop propagation for direct connections, the multi-hop propagation estimates the information dissemination ability, i.e., informativeness of each vertex, more accurately. In Fig. 4, the one-hop cost of information propagation from A to vertices (B, C) and D to (E, F) is the same for the left and right graphs, although in the left graph C can be learned more effectively through B instead of directly from A . The two-hop propagation can be naturally extended to multi-hop propagation by exploring higher order neighbors. For simplicity and efficiency, we only explore up to two-hop.

K -Means clustering for diversity and coverage. In addition to each instance being representative of its individual neighborhood, we also want to select diversified instances that collectively capture the structure of the entire unlabeled data. Thus, we perform K -Means clustering that partitions the n instances into m ($\leq n$) clusters $\mathbb{S} = \{S_1, S_2, \dots, S_m\}$ in which each instance belongs to the cluster with nearest cluster centroid μ that serves as a prototype of the cluster [24, 45]. The objective is to find \mathbb{S} that minimizes the within-cluster sum of squares (WCSS) [39]:

$$\arg \min_{\mathbb{S}} \sum_{i=1}^m \sum_{V \in S_i} \|V - \mu_i\|^2 = \arg \min_{\mathbb{S}} \sum_{i=1}^m |S_i| \text{Var}(S_i) \quad (5)$$

In our case, m is approximately equal to annotation budget. The m centroids of K -Means clustering are randomly initialized and optimized with the EM algorithm [47].

We then select the instance with the highest utility score evaluated according to Eqn. 4 from each cluster.

Regularization with inter-cluster information passing channels. Even with the hard constraints from K -Means clustering, sometimes our instance sampler still selects samples very close to other selected samples in adjacent regions (Fig. 5), especially when the densest area in a cluster is at a corner or boundary, causing insufficient overall diversity.

To avoid such repetitive sampling that reduces the total information carried in the labeled set, we apply soft constraints through an iterated regularization algorithm.

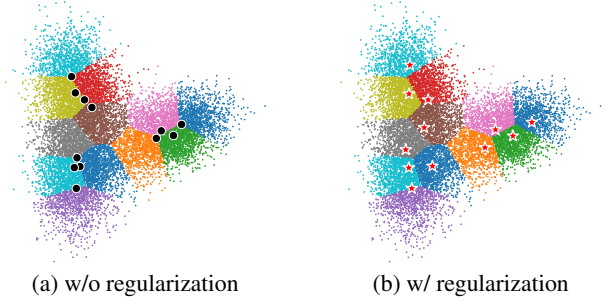


Figure 5. Sampling with regularization (right) can produce more uniform and diversified queries. On the contrary, the queries acquired without regularization (left) are usually located in a small dense region and have high correlations, losing the overall representativeness. (better viewed in color)

At each iteration, different clusters exchange information about other clusters’ selected samples and gradually adjust their selections for better diversity and coverage. Specifically, after the original sample selection, we compute a regularizer $\text{Reg}(V_i, t)$ for each sample V_i based on the distance from each candidate to the whole selected query set $\hat{\mathbb{V}}^{t-1} = \{\hat{V}_1^{t-1}, \dots, \hat{V}_m^{t-1}\}$ at iteration $t-1$, except for the query in the same cluster S_i , with a tunable strength hyperparameter α :

$$\text{Reg}(V_i, t) = \sum_{\hat{V}_j^{t-1} \notin S_i} \frac{1}{\|V_i - \hat{V}_j^{t-1}\|^\alpha} \quad (6)$$

The regularizer is updated with an exponential moving average with momentum m_{reg} :

$$\bar{\text{Reg}}(V_i, t) = m_{\text{reg}} \bar{\text{Reg}}(V_i, t-1) + (1 - m_{\text{reg}}) \text{Reg}(V_i, t) \quad (7)$$

After that, at iteration t , we select sample i with maximum **regularized utility** $U'(V_i, t)$ in each cluster, formulated as:

$$U'(V_i, t) = U(V_i) - \lambda \cdot \bar{\text{Reg}}(V_i, t) \quad (8)$$

where λ is a hyperparameter that controls the trade-off between diversity and informativeness: A low λ leads to samples close to each other and of low diversity; a high λ leads to uniformly distributed samples of low informativeness. The selection formed at the last iteration is our final choice. By adding a soft regularization, this formulation does not just push data point selections away to a certain distance, but it considers the trade-off between diversity and representativeness and attempts to find another mode in the cluster for potentially new information if labeled, thus greatly enhancing the overall informativeness. We refer readers to Appendix for pseudo-code of the regularization algorithm.

In large datasets, calculating the distances between a sample and all queries in $\hat{\mathbb{V}}^{t-1}$ is no longer feasible. Fortunately, only selected samples that are close to the current candidate make a big difference in $\text{Reg}(V_i, t)$. Therefore, we set a horizon h , defined as the number of nearest

neighbor selections from \hat{V}^{t-1} to be considered, for large datasets. We found that h ranging from 32 to 128 generally works well in our experiments.

Acceleration with general-domain multi-modal models.

We further improve our method on two aspects: 1) We need to train a self-supervised model for each new dataset, which is time-consuming and could potentially delay data annotation in real-world applications. 2) Self-supervised methods do not model semantic information explicitly, and datasets with varying intra-class variance assume regions of various sizes and may be treated in an unexpected way. To address these issues, we resort to a large pretrained model that encodes semantics without manual human annotation.

We make use of publicly-available CLIP [50] models, a collection of models trained on Internet-crawled large-scale data with a wide general domain, and use CLIP’s image model as feature extractor. We observe that such substitution does not hurt and even helps the performance when annotation budget is large when compared to self-supervised models, demonstrating the effectiveness of making use of semantic information. Since we do not need to train models with the target dataset, the whole sample selection process could complete in *0.5 hours* on a commodity server with one GPU, which illustrates the possibility of our method without delaying the human annotation schedule or modifying the annotation pipeline to wait for self-supervised models in real-world dataset collection in the industry. More discussions on CLIP can be found in Appendix.

4. Experiments

In this section, we perform a comprehensive evaluation on the proposed Data-Centric Semi-Supervised Learning (DC-SSL) integrated with several mainstream SSL approaches: pseudo-label based FixMatch [59], MixMatch [4], CoMatch [43] and transfer-learning based SimCLRv2-CLD, which fine-tunes a model pretrained with self-supervised method CLD [63] in the way proposed by SimCLRv2 [12]. In addition to SSL, we also compare with AL and SSAL methods. We conducted analysis on key properties of our methods and found several surprising characteristics including label efficiency, stability, and generalizability.

4.1. CIFAR-10

Setup. We evaluate FixMatch [59] and SimCLRv2-CLD [12, 63] on low-shot settings from 40 samples to 250 samples in total (4 to 25 shots per class on average). In addition, we also present MixMatch [4] and recently-proposed CoMatch [43] for a comprehensive comparison. For fair comparison, we re-evaluate baseline methods with random sampling. Note that the self-supervised model used for sample selection is only trained on CIFAR-10 with *no external data*. All FixMatch, MixMatch, and CoMatch models are trained from scratch, while SimCLRv2-CLD reuses the

Sampling Method	Accuracy (%)		
	40 labels	100 labels	250 labels
Random	82.94 ± 9.77	88.72 ± 4.61	93.28 ± 0.04
DC-SSL (Ours)	91.10 ± 0.95	93.22 ± 0.31	93.63 ± 0.14
Δ	↑ 8.16	↑ 4.50	↑ 0.35 ‡
Stratified †	88.61 ± 3.35	90.19 ± 2.24	94.93 ± 0.33

Table 2. DC-SSL greatly outperforms random sampling: CIFAR-10 experiments with FixMatch [59] using 3 different folds. † is not a fair comparison with us because it assumes balanced labeled data available and leaks information about ground truth labels. ‡: The 0.35% improvement in 250 label task is *not marginal*, since 250 labels to 4000 labels (16×) only leads to around 0.7% improvement as reported in FixMatch. Δ : gains over Random.

Sampling Method	SimCLRv2-CLD	MixMatch	CoMatch
Random	60.8 ± 3.2	43.6 ± 3.4	85.0 ± 1.6
DC-SSL (Ours)	76.3 ± 1.6	64.2 ± 4.2	93.7 ± 0.8
Δ	↑ 15.5	↑ 20.6	↑ 8.7
Stratified †	74.5 ± 0.8	62.0 ± 0.5	93.1 ± 1.4

Table 3. DC-SSL is a universal framework that works with various SSL methods: CIFAR-10 experiments with SimCLRv2-CLD [12, 63], MixMatch [4], and CoMatch [43] using 40 labeled samples. SimCLRv2-CLD results are with 5 different folds and 2 runs in each fold. MixMatch and CoMatch are with 3 and 2 folds, respectively. †: we outperform stratified sampling even though it uses external information. Δ : gains over Random.

CLD model for sample selection. Since our work is data-centric, we follow the same training recipe unless stated. Detailed setup is in Appendix.

Main results. FixMatch. In Table 2, two charming properties of DC-SSL are observed in the CIFAR-10 experiments: *label efficiency and stability*. In addition to consistently improving on previous methods, we also found that two of the first 5 seeds of random selection have labels from fewer than 10 classes in 40 samples task, whereas it does not occur in our method, even when we sample *100 times* with 100 seeds. We skip the seeds with under-coverage in random selection to better understand the improvements of our methods, but this will be nearly impossible in reality. In 250 samples task, although FixMatch already performs well, we are able to push the limit further by a small amount. Furthermore, in low-shot SSL tasks with random sampling, we observe a collapsing effect that the validation accuracy drops drastically in the training process and does not climb back, which is due to unrepresentative samples misleading the network into classifying a range of samples to a wrong class, which further generates wrong pseudo-labels and creates confirmation bias. To quantify this effect, we calculate the accuracy gap between the best and the last epoch. We found that the accuracy from the best epoch is 3.73% higher than the accuracy from the last epoch in 40 labels task, even after taking the mean of 3 different folds. In comparison, our method reduces this gap to 0.17% by selecting labels

Sampling Method	Supervised Learning		Semi-supervised Learning	
	1%	0.20%	1%	0.20%
Random	23.5	6.0	58.8	34.3
DC-SSL with MoCo (Ours)	24.7 \uparrow 1.2	9.2 \uparrow 3.2	61.6 \uparrow 2.8	48.6 \uparrow 14.3
DC-SSL with CLIP (Ours)	27.3 \uparrow 3.8	9.7 \uparrow 3.7	62.2 \uparrow 3.4	47.5 \uparrow 13.2
Stratified \dagger	22.9	6.3	60.9*	41.1

Table 4. DC-SSL scales well on large-scale dataset ImageNet with fully supervised training and SSL algorithm FixMatch [59] with EMAN [7]. * indicates results reported in EMAN. Note that \dagger is not a fair comparison, as explained earlier.

that are representative and diverse (see Appendix for details).

SimCLRv2-CLD, MixMatch, and CoMatch. In Table 3, since SimCLRv2-CLD only considers labeled samples in the fine-tuning stage, the quality of the trained classifier greatly depends on selected samples’ quality when compared to FixMatch. In 40 labels settings, we are able to achieve an astonishing 15.5% improvement. In MixMatch, we achieve an absolute improvement of 20.6% over baseline. Although our method has a larger variance between folds than baseline, our method performs at least 16% better *on every fold*. In CoMatch, which already has high label efficiency, we still improve 8.7% over random sampling.

4.2. ImageNet

Setup. To further evaluate the effectiveness of our method on large-scale datasets with more classes. We perform evaluation of our method on ImageNet [53] with about 1.28M images and 1k classes. We perform supervised learning (SL) and SSL on both 1% labeled data (12820 samples) and 0.2% (2911 samples). Following [7], we initialize our parameters in FixMatch with a MoCov2 model trained for 800 epochs for fair comparison. Detailed setup is in Appendix.

Main results. As summarized in Table 6, samples selected from both MoCo and CLIP models boost the performance of SL and SSL. In the 1% case, DC-SSL provides 1.2% to 3.8% (2.8% to 3.4%) gains in the SL (SSL) setting. What is more interesting is the 0.2% setting, where our method leads to an improvement ranging from 13.2% to 14.3% in SSL. We found that samples selected from MoCo perform 1.1% better than samples from CLIP in the FixMatch setting. This is, in part, due to mismatch between parameter initialization (MoCo) and the feature space used for the sampling process (CLIP). However, for 1% case, we find that this dependency disappears and samples with CLIP perform 0.6% better than MoCo, which demonstrates the benefits of using a model with explicit semantic information during pretraining with sufficient general knowledge.

4.3. Generality of sample selection process

Generality in results with CLIP. Since CLIP *does not use ImageNet samples* in training and the downstream SSL task *has never seen the CLIP model* in training either, we stress the importance of *generality*: it means that **1**) when a new dataset is collected, we could use a general model with

Sampling Method	Accuracy (%)
Random	77.17 \pm 6.98
DC-SSL (Ours)	88.06 \pm 1.41 \uparrow 10.89
Stratified \dagger	80.46 \pm 7.88

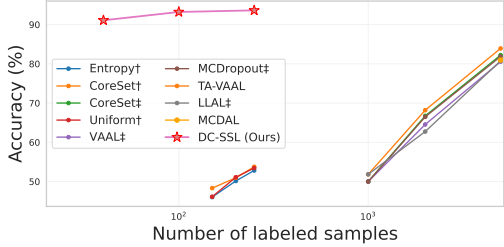
Table 5. DC-SSL shows remarkable generalizability across domains: BloodMNIST [69] experiments with FixMatch [59] on 3 different folds and 40 labeled instances (5-shot on average per class). Annotated samples are chosen by a self-supervised CLD model trained only on CIFAR-10 and is *never trained on medical images*. We adopt the same settings as FixMatch on CIFAR-10, except that we train only for 64 epochs for best performance. \dagger : outperforming stratified sampling with less information.

knowledge of the target domain to select samples without waiting for self-supervised learning (see Sec. 4.5); **2**) different from active learning, where sample selection process is strictly coupled with training, our annotated dataset works *universally* rather than only with the model used to select it. **Cross-domain generality.** To further analyze whether such generality also holds across domains, we use the exact same CLD model pretrained on CIFAR-10 to select samples in the BloodMNIST dataset of the MedMNISTv2 collection [69] for annotation. BloodMNIST contains about 18k blood cell images under microscope in 8 classes, which is drastically different from CIFAR-10’s domain, yet as shown in Table 5, our model with FixMatch performs 10.89% better than random sampling and 7.6% better than stratified sampling, further illustrating the possibility of a general sample selection model.

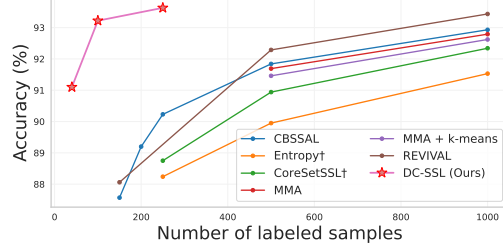
4.4. Comparison with AL and SSAL Methods

One main difference between our work and previous AL/SSAL works is that we select samples to label *only once*, without any prior information of downstream classification tasks. This puts us at disadvantage, because we will not be able to improve future label selection based on feedback from previous rounds. However, we still outperform previous AL/SSAL algorithms with higher label efficiency, as shown in Fig. 6, partially because of the elimination of inefficient initial random selection in AL/SSAL methods.

We first compare our work with previous AL methods. Since AL only utilizes labeled samples, even recent AL algorithms such as [14] requires at least 10,000 samples to achieve 90% accuracy (250 \times more than ours). To compare fairly with AL, we attempt to use AL to select 20 samples with 20 initial random samples and then utilize the 40 sam-



(a) Comparison with AL Methods



(b) Comparison with SSAL Methods

Figure 6. We compare our work with AL methods [14, 25, 38, 55, 58, 71] and SSAL methods [26, 31, 60]. Our method outperforms both AL and SSAL methods with a much higher sample efficiency. Note that although MMA also experimented with k-Means, it does not benefit their performance. †: results from [26]. ‡: results from [38].

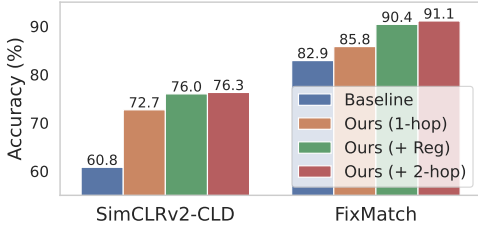


Figure 7. Illustration of our methods with different ablations on CIFAR-10 with 40 samples. In both methods, applying 1-hop propagation gives large improvements, and regularization as well as 2-hop propagation together give additional small improvements.

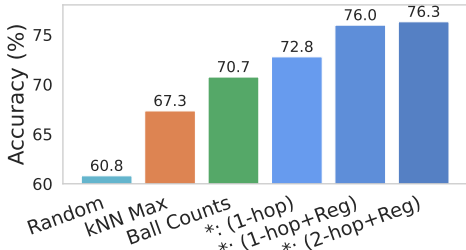


Figure 8. The effect of different utility estimations on SimCLRv2-CLD. *kNN Max* is vanilla *K*-NN density estimation that takes the max distance of *K* nearest-neighbors. *Ball Counts* counts neighbors within a radius. Our methods (with *): *1-hop* is our method without regularization or second order term. *1-hop+Reg* adds regularization and *2-hop+Reg* adds a second order propagation.

ples in SSL. However, since 20 is smaller than batch size 128, our LLAL [71] implementation has about 20% accuracy. Therefore, naively using AL for SSL sample selection does not serve as a useful comparison. Therefore, we also compare with SSAL which is specifically designed for combining AL and SSL and inherits both approaches’ advantages. Similar to our work, SSAL [26, 31, 60] uses unlabeled samples with AL methods. However, SSAL still requires initial annotation from random sampling, which inherits its inefficiency on low-shot selection (as shown in Fig. 2 (b)). In contrast, our method could select samples efficiently. We believe that it is possible to further improve our work if we use DC-SSL for initial selection in SSAL, but we leave it to future work due to the complexity of both algorithms. See Appendix for more comparisons with AL/SSAL.

4.5. Ablation Study and Detailed Analysis

Component Analysis. To investigate contributions of each component, we evaluate our method with an extensive ablation study. Illustrated in Fig. 7, applying the vanilla version of our method based on first order scores achieves large improvements on both SSL methods, especially SimCLRv2-CLD where the accuracy rises by 11.9%. Adding regularization improves 4.6% (FixMatch) and 3.3% (SimCLRv2-CLD) by contributing to sample diversity. In the end, 2-hop propagation leads to another marginal 0.7% and 0.3% improvement on both methods. These contributions together lead to our final 8.2% and 15.5% improvement.

Formulation Analysis. We systematically evaluated variants of representativeness estimation formulations, by comparing different ablations of our methods to other metrics (Fig. 8). We compare against two common metrics: *KNN Max* (vanilla *K*-NN) and *Ball Counts* (neighbor counts within a radius). Although all three methods are much better than random selection, ours leads to the best outcome.

Run Time Analysis. We only add a negligible delay to label selection compared to SSL methods. On ImageNet, we only introduce less than 1 GPU hour overhead when compared to about 2300 GPU hours with the original FixMatch pipeline. With CLIP, the data selection stage could start as soon as data is available, which enables informative labeling with very low delay.

More ablation studies on **hyperparameters**, **run time analysis**, and **visualizations of selections** are in Appendix.

5. Summary

In contrast to existing model-centric SSL methods that focus on models and algorithms that integrate both labeled and unlabeled data, our DC-SSL is the first work that turns focus to an unsupervised labeled data selection in SSL. By choosing a representative and diverse set of samples for annotation, we demonstrate significant gains on annotation efficiency, model stability and accuracy on all experimented benchmarks with generality of sample selection within and across domains. We are committed to a public code release,

and we believe our work will facilitate research on future data-centric methods.

References

- [1] Dana Angluin. Queries and concept learning. *Machine learning*, 2(4):319–342, 1988. [3](#)
- [2] Les E Atlas, David A Cohn, and Richard E Ladner. Training connectionist networks with queries and selective sampling. In *Advances in neural information processing systems*, pages 566–573. Citeseer, 1990. [3](#)
- [3] David Berthelot, Nicholas Carlini, Ekin D Cubuk, Alex Kurakin, Kihyuk Sohn, Han Zhang, and Colin Raffel. Remixmatch: Semi-supervised learning with distribution alignment and augmentation anchoring. *arXiv preprint arXiv:1911.09785*, 2019. [1](#), [3](#), [6](#)
- [4] David Berthelot, Nicholas Carlini, Ian Goodfellow, Nicolas Papernot, Avital Oliver, and Colin Raffel. Mixmatch: A holistic approach to semi-supervised learning. *arXiv preprint arXiv:1905.02249*, 2019. [1](#), [3](#), [6](#)
- [5] Mustafa Bilgic and Lise Getoor. Link-based active learning. In *NIPS Workshop on Analyzing Networks and Learning with Graphs*, volume 4, 2009. [3](#)
- [6] John Adrian Bondy, Uppaluri Siva Ramachandra Murty, et al. *Graph theory with applications*, volume 290. Macmillan London, 1976. [4](#)
- [7] Zhaowei Cai, Avinash Ravichandran, Subhransu Maji, Charles Fowlkes, Zhuowen Tu, and Stefano Soatto. Exponential moving average normalization for self-supervised and semi-supervised learning. In *Proceedings of the IEEE/CVF Conference on Computer Vision and Pattern Recognition*, pages 194–203, 2021. [4](#), [7](#), [12](#), [14](#), [16](#)
- [8] Nicholas Carlini, Ulfar Erlingsson, and Nicolas Papernot. Distribution density, tails, and outliers in machine learning: Metrics and applications. *arXiv preprint arXiv:1910.13427*, 2019. [3](#)
- [9] Mathilde Caron, Piotr Bojanowski, Armand Joulin, and Matthijs Douze. Deep clustering for unsupervised learning of visual features. In *ECCV*, 2018. [3](#)
- [10] Mathilde Caron, Ishan Misra, Julien Mairal, Priya Goyal, Piotr Bojanowski, and Armand Joulin. Unsupervised learning of visual features by contrasting cluster assignments. *Advances in Neural Information Processing Systems*, 33, 2020. [3](#)
- [11] Ting Chen, Simon Kornblith, Mohammad Norouzi, and Geoffrey Hinton. A simple framework for contrastive learning of visual representations. In *International conference on machine learning*, pages 1597–1607. PMLR, 2020. [3](#), [4](#)
- [12] Ting Chen, Simon Kornblith, Kevin Swersky, Mohammad Norouzi, and Geoffrey Hinton. Big self-supervised models are strong semi-supervised learners. *arXiv preprint arXiv:2006.10029*, 2020. [1](#), [3](#), [6](#), [11](#), [12](#), [14](#), [15](#)
- [13] Xinlei Chen, Haoqi Fan, Ross Girshick, and Kaiming He. Improved baselines with momentum contrastive learning. *arXiv preprint arXiv:2003.04297*, 2020. [4](#), [12](#)
- [14] Jae Won Cho, Dong-Jin Kim, Yunjae Jung, and In So Kweon. Mcdal: Maximum classifier discrepancy for active learning. *arXiv preprint arXiv:2107.11049*, 2021. [7](#), [8](#)
- [15] Fan RK Chung and Fan Chung Graham. *Spectral graph theory*. Number 92. American Mathematical Soc., 1997. [4](#)
- [16] David Cohn, Les Atlas, and Richard Ladner. Improving generalization with active learning. *Machine learning*, 15(2):201–221, 1994. [3](#)
- [17] Ronan Collobert, Jason Weston, Léon Bottou, Michael Karlen, Koray Kavukcuoglu, and Pavel Kuksa. Natural language processing (almost) from scratch. *Journal of machine learning research*, 12(ARTICLE):2493–2537, 2011. [1](#)
- [18] Ekin D Cubuk, Barret Zoph, Jonathon Shlens, and Quoc V Le. Randaugment: Practical automated data augmentation with a reduced search space. In *Proceedings of the IEEE/CVF Conference on Computer Vision and Pattern Recognition Workshops*, pages 702–703, 2020. [3](#)
- [19] Ido Dagan and Sean P Engelson. Committee-based sampling for training probabilistic classifiers. In *Machine Learning Proceedings 1995*, pages 150–157. Elsevier, 1995. [3](#)
- [20] N Deo. Graph theory with applications to engineering and computer science. *Networks*, 5(3):299–300, 1975. [4](#)
- [21] Alexey Dosovitskiy, Lucas Beyer, Alexander Kolesnikov, Dirk Weissenborn, Xiaohua Zhai, Thomas Unterthiner, Mostafa Dehghani, Matthias Minderer, Georg Heigold, Sylvain Gelly, et al. An image is worth 16x16 words: Transformers for image recognition at scale. *arXiv preprint arXiv:2010.11929*, 2020. [16](#)
- [22] Melanie Ducoffe and Frederic Precioso. Adversarial active learning for deep networks: a margin based approach. *arXiv preprint arXiv:1802.09841*, 2018. [3](#)
- [23] Evelyn Fix and Joseph Lawson Hodges. Discriminatory analysis. nonparametric discrimination: Consistency properties. *International Statistical Review/Revue Internationale de Statistique*, 57(3):238–247, 1989. [4](#)
- [24] Edward W Forgy. Cluster analysis of multivariate data: efficiency versus interpretability of classifications. *biometrics*, 21:768–769, 1965. [5](#)
- [25] Yarin Gal, Riashat Islam, and Zoubin Ghahramani. Deep bayesian active learning with image data. In *International Conference on Machine Learning*, pages 1183–1192. PMLR, 2017. [8](#)
- [26] Mingfei Gao, Zizhao Zhang, Guo Yu, Sercan Ö Arık, Larry S Davis, and Tomas Pfister. Consistency-based semi-supervised active learning: Towards minimizing labeling cost. In *European Conference on Computer Vision*, pages 510–526. Springer, 2020. [3](#), [8](#), [13](#)
- [27] Ross Girshick, Jeff Donahue, Trevor Darrell, and Jitendra Malik. Rich feature hierarchies for accurate object detection and semantic segmentation. In *Proceedings of the IEEE conference on computer vision and pattern recognition*, pages 580–587, 2014. [1](#)
- [28] Ian Goodfellow, Yoshua Bengio, and Aaron Courville. *Deep learning*. MIT press, 2016. [1](#)
- [29] Yves Grandvalet, Yoshua Bengio, et al. Semi-supervised learning by entropy minimization. *CAP*, 367:281–296, 2005. [1](#), [3](#)
- [30] Jean-Bastien Grill, Florian Strub, Florent Altché, Corentin Tallec, Pierre H Richemond, Elena Buchatskaya, Carl Doersch, Bernardo Avila Pires, Zhaohan Daniel Guo, Mohammad Gheshlaghi Azar, et al. Bootstrap your own latent: A

- new approach to self-supervised learning. *arXiv preprint arXiv:2006.07733*, 2020. 3
- [31] Jiannan Guo, Haochen Shi, Yangyang Kang, Kun Kuang, Siliang Tang, Zhuoren Jiang, Changlong Sun, Fei Wu, and Yueting Zhuang. Semi-supervised active learning for semi-supervised models: Exploit adversarial examples with graph-based virtual labels. In *Proceedings of the IEEE/CVF International Conference on Computer Vision*, pages 2896–2905, 2021. 8
- [32] Raia Hadsell, Sumit Chopra, and Yann LeCun. Dimensionality reduction by learning an invariant mapping. In *CVPR*, 2006. 12
- [33] Kaiming He, Haoqi Fan, Yuxin Wu, Saining Xie, and Ross Girshick. Momentum contrast for unsupervised visual representation learning. In *Proceedings of the IEEE/CVF Conference on Computer Vision and Pattern Recognition*, pages 9729–9738, 2020. 3, 4, 14, 16
- [34] Kaiming He, Xiangyu Zhang, Shaoqing Ren, and Jian Sun. Deep residual learning for image recognition. In *Proceedings of the IEEE conference on computer vision and pattern recognition*, pages 770–778, 2016. 11
- [35] Joel Hestness, Sharan Narang, Newsha Ardalani, Gregory Diamos, Heewoo Jun, Hassan Kianinejad, Md Patwary, Mostofa Ali, Yang Yang, and Yanqi Zhou. Deep learning scaling is predictable, empirically. *arXiv preprint arXiv:1712.00409*, 2017. 1
- [36] Sheng-Jun Huang, Rong Jin, and Zhi-Hua Zhou. Active learning by querying informative and representative examples. *Advances in neural information processing systems*, 23:892–900, 2010. 3
- [37] Sergey Ioffe and Christian Szegedy. Batch normalization: Accelerating deep network training by reducing internal covariate shift. In *International conference on machine learning*, pages 448–456. PMLR, 2015. 12
- [38] Kwanyoung Kim, Dongwon Park, Kwang In Kim, and Se Young Chun. Task-aware variational adversarial active learning. In *Proceedings of the IEEE/CVF Conference on Computer Vision and Pattern Recognition*, pages 8166–8175, 2021. 8
- [39] Hans-Peter Kriegel, Erich Schubert, and Arthur Zimek. The (black) art of runtime evaluation: Are we comparing algorithms or implementations? *Knowledge and Information Systems*, 52(2):341–378, 2017. 5
- [40] Alex Krizhevsky, Ilya Sutskever, and Geoffrey E Hinton. Imagenet classification with deep convolutional neural networks. *Advances in neural information processing systems*, 25:1097–1105, 2012. 1
- [41] Yann LeCun, Yoshua Bengio, and Geoffrey Hinton. Deep learning. *nature*, 521(7553):436–444, 2015. 1
- [42] Dong-Hyun Lee et al. Pseudo-label: The simple and efficient semi-supervised learning method for deep neural networks. In *Workshop on challenges in representation learning, ICML*, volume 3, 2013. 1, 3
- [43] Junnan Li, Caiming Xiong, and Steven CH Hoi. Comatch: Semi-supervised learning with contrastive graph regularization. In *Proceedings of the IEEE/CVF International Conference on Computer Vision*, pages 9475–9484, 2021. 6
- [44] Bin Liu, Zhirong Wu, Han Hu, and Stephen Lin. Deep metric transfer for label propagation with limited annotated data. In *Proceedings of the IEEE/CVF International Conference on Computer Vision Workshops*, pages 0–0, 2019. 3
- [45] Stuart Lloyd. Least squares quantization in pcm. *IEEE transactions on information theory*, 28(2):129–137, 1982. 5
- [46] Don O Loftsgaarden and Charles P Quesenberry. A non-parametric estimate of a multivariate density function. *The Annals of Mathematical Statistics*, 36(3):1049–1051, 1965. 4
- [47] Geoffrey J McLachlan and Thriyambakam Krishnan. *The EM algorithm and extensions*, volume 382. John Wiley & Sons, 2007. 5
- [48] Aaron van den Oord, Yazhe Li, and Oriol Vinyals. Representation learning with contrastive predictive coding. *arXiv preprint arXiv:1807.03748*, 2018. 4, 12
- [49] Jan Orava. K-nearest neighbour kernel density estimation, the choice of optimal k. *Tatra Mountains Mathematical Publications*, 50(1):39–50, 2011. 4
- [50] Alec Radford, Jong Wook Kim, Chris Hallacy, Aditya Ramesh, Gabriel Goh, Sandhini Agarwal, Girish Sastry, Amanda Askell, Pamela Mishkin, Jack Clark, et al. Learning transferable visual models from natural language supervision. *arXiv preprint arXiv:2103.00020*, 2021. 6, 13
- [51] Pengzhen Ren, Yun Xiao, Xiaojun Chang, Po-Yao Huang, Zhihui Li, Xiaojiang Chen, and Xin Wang. A survey of deep active learning. *arXiv preprint arXiv:2009.00236*, 2020. 3
- [52] Nicholas Roy and Andrew McCallum. Toward optimal active learning through sampling estimation of error reduction. *Proceedings of the 18th International Conference on Machine Learning*, 08 2001. 3
- [53] Olga Russakovsky, Jia Deng, Hao Su, Jonathan Krause, Sanjeev Satheesh, Sean Ma, Zhiheng Huang, Andrej Karpathy, Aditya Khosla, Michael Bernstein, Alexander C. Berg, and Li Fei-Fei. ImageNet Large Scale Visual Recognition Challenge. *International Journal of Computer Vision (IJCV)*, 115(3):211–252, 2015. 7, 16
- [54] Mehdi Sajjadi, Mehran Javanmardi, and Tolga Tasdizen. Regularization with stochastic transformations and perturbations for deep semi-supervised learning. *arXiv preprint arXiv:1606.04586*, 2016. 1, 3
- [55] Ozan Sener and Silvio Savarese. Active learning for convolutional neural networks: A core-set approach. *arXiv preprint arXiv:1708.00489*, 2017. 3, 8, 13
- [56] Burr Settles. Active learning literature survey. 2009. 3
- [57] Jianbo Shi and Jitendra Malik. Normalized cuts and image segmentation. *IEEE Transactions on pattern analysis and machine intelligence*, 22(8):888–905, 2000. 4
- [58] Samarth Sinha, Sayna Ebrahimi, and Trevor Darrell. Variational adversarial active learning. In *Proceedings of the IEEE/CVF International Conference on Computer Vision*, pages 5972–5981, 2019. 8
- [59] Kihyuk Sohn, David Berthelot, Nicholas Carlini, Zizhao Zhang, Han Zhang, Colin A Raffel, Ekin Dogus Cubuk, Alexey Kurakin, and Chun-Liang Li. Fixmatch: Simplifying semi-supervised learning with consistency and confidence. *Advances in Neural Information Processing Systems*, 33, 2020. 1, 3, 4, 6, 7, 11, 14, 15, 16

- [60] Shuang Song, David Berthelot, and Afshin Rostamizadeh. Combining mixmatch and active learning for better accuracy with fewer labels. *arXiv preprint arXiv:1912.00594*, 2019. [3](#), [8](#), [13](#)
- [61] Antti Tarvainen and Harri Valpola. Mean teachers are better role models: Weight-averaged consistency targets improve semi-supervised deep learning results. In *Proceedings of the 31st International Conference on Neural Information Processing Systems*, pages 1195–1204, 2017. [1](#), [3](#)
- [62] Simon Tong and Daphne Koller. Support vector machine active learning with applications to text classification. *Journal of machine learning research*, 2(Nov):45–66, 2001. [3](#)
- [63] Xudong Wang, Ziwei Liu, and Stella X Yu. Unsupervised feature learning by cross-level instance-group discrimination. In *Proceedings of the IEEE/CVF Conference on Computer Vision and Pattern Recognition*, pages 12586–12595, 2021. [1](#), [3](#), [4](#), [6](#), [12](#), [13](#), [14](#), [15](#)
- [64] Kai Wei, Rishabh Iyer, and Jeff Bilmes. Submodularity in data subset selection and active learning. In *International Conference on Machine Learning*, pages 1954–1963. PMLR, 2015. [3](#)
- [65] Zhirong Wu, Yuanjun Xiong, Stella X Yu, and Dahua Lin. Unsupervised feature learning via non-parametric instance discrimination. In *Proceedings of the IEEE Conference on Computer Vision and Pattern Recognition*, pages 3733–3742, 2018. [3](#), [4](#)
- [66] Junyuan Xie, Ross Girshick, and Ali Farhadi. Unsupervised deep embedding for clustering analysis. In *ICML*, 2016. [3](#)
- [67] Qizhe Xie, Zihang Dai, Eduard Hovy, Thang Luong, and Quoc Le. Unsupervised data augmentation for consistency training. *Advances in Neural Information Processing Systems*, 33, 2020. [1](#), [3](#)
- [68] Qizhe Xie, Minh-Thang Luong, Eduard Hovy, and Quoc V Le. Self-training with noisy student improves imagenet classification. In *Proceedings of the IEEE/CVF Conference on Computer Vision and Pattern Recognition*, pages 10687–10698, 2020. [1](#)
- [69] Jiancheng Yang, Rui Shi, Donglai Wei, Zequan Liu, Lin Zhao, Bilian Ke, Hanspeter Pfister, and Bingbing Ni. Medmnist v2: A large-scale lightweight benchmark for 2d and 3d biomedical image classification. *arXiv preprint arXiv:2110.14795*, 2021. [7](#)
- [70] Yi Yang, Dong Xu, Feiping Nie, Shuicheng Yan, and Yueting Zhuang. Image clustering using local discriminant models and global integration. *TIP*, 2010. [3](#)
- [71] Donggeun Yoo and In So Kweon. Learning loss for active learning. In *Proceedings of the IEEE/CVF Conference on Computer Vision and Pattern Recognition*, pages 93–102, 2019. [3](#), [8](#)
- [72] Yang You, Igor Gitman, and Boris Ginsburg. Large batch training of convolutional networks. *arXiv preprint arXiv:1708.03888*, 2017. [11](#)
- [73] Chengxu Zhuang, Alex Lin Zhai, Daniel Yamins, , et al. Local aggregation for unsupervised learning of visual embeddings. In *ICCV*, 2019. [3](#)

A. Appendix

A.1. Pseudo-code for Regularization Algorithm

We summarized the regularization algorithm in pseudo-code in Alg. 1. In Alg. 1, we first obtain $\hat{\mathbb{V}}^0$, the selection without regularization, and set the moving average regularizer $\text{Reg}(V_i, 0)$ to 0 for every $V_i \in \mathbb{V}$; then in each iteration, we update $\text{Reg}(V_i, t)$ with moving average from a closeness measurement to other previously selected samples, where t is the index of current iteration. We re-select samples according to regularized utility at the end of each iteration, with λ being a balancing factor. In the end, the selection from the last iteration is returned.

A.2. Our Method with SimCLRv2 on ImageNet

In addition to FixMatch [59] and supervised learning on ImageNet, we also adapt our method to SimCLRv2 [12].

Setup. We fine-tune the released SimCLRv2 checkpoint on baseline selections and our selections. Due to differences in codebases, our reproduced accuracy differs from the one reported on SimCLRv2 paper pretrained and fine-tuned on Cloud TPUs. Therefore, we will also report reproduced baseline which is fine-tuned on stratified selection for comparison on the effectiveness on sample selection with our method with SimCLRv2. Similar to other ImageNet experiments, we use 1% and 0.2% labeled data. The labeled data selection is the same for SimCLRv2 as for our experiments in FixMatch. To keep the recipe as close to the original implementation as possible, we use ResNet-50 [34] with LARS [72] optimizer with learning rate 0.16 and use glob-

Algorithm 1 The iterative regularization algorithm

Require:

$\{U(V_i) | V_i \in \mathbb{V}\}$: The unregularized utility for each vertex V_i

λ : weight for applying regularization

m_{reg} : momentum in exponential moving average

l : the number of iterations

Procedure:

$\bar{\text{Reg}}(V_i, 0) \leftarrow 0, \forall V_i \in \mathbb{V}$

$\hat{\mathbb{V}}^0 \leftarrow$ samples with largest $U(V_i)$ in each cluster

for $t = 1$ **to** l **do**

for all $V_i \in \mathbb{V}$ **do**

$\text{Reg}(V_i, t) \leftarrow \sum_{\hat{V}_j^{t-1} \notin \mathcal{S}_i} \frac{1}{\|V_i - \hat{V}_j^{t-1}\|^\alpha}$

$\bar{\text{Reg}}(V_i, t) \leftarrow m_{\text{reg}} \cdot \bar{\text{Reg}}(V_i, t-1) + (1 - m_{\text{reg}}) \cdot$

$\text{Reg}(V_i, t)$

$U'(V_i, t) \leftarrow U(V_i) - \lambda \cdot \bar{\text{Reg}}(V_i, t)$

end for

$\hat{\mathbb{V}}^t \leftarrow$ samples with largest $U'(V_i, t)$ in each cluster

end for

return $\hat{\mathbb{V}}^l$

Sampling Method	1%		0.2%	
	1× Schedule	2× Schedule	1× Schedule	2× Schedule
Random	49.7	52.8	28.1	33.2
DC-SSL with MoCo (Ours)	51.5 ↑ 1.8	54.0 ↑ 1.2	33.0 ↑ 4.9	39.8 ↑ 6.6
DC-SSL with CLIP (Ours)	52.6 ↑ 2.9	54.2 ↑ 1.4	35.4 ↑ 7.3	41.2 ↑ 8.0
Stratified (reproduced) †	52.0	53.8	33.7	37.4
Stratified (reported in [12]) †	57.9	-	-	-

Table 6. DC-SSL scales well on large-scale dataset ImageNet with SimCLRv2 [12]. Note that † is not a fair comparison, as explained earlier. Our method improves up to 8.0% (2.9%) when compared to baseline with 0.2% (1%) labeled data.

ally synced batch normalization [37]. While [12] employs a batch size of 1024, we found that under the same number of training epochs, setting batch size to 512 leads to better optimization outcomes in our codebase. This is potentially due to more iterations with the same number of training epochs. Therefore, we set batch sizes in all experiments to 512. In addition, to reduce the memory footprint, we use mixed precision training, which has no significant impacts in training accuracy in our observation. We use 60 epochs as 1× schedule for 1% task, following [12] and 120 epochs as 1× schedule for 0.2% task. However, we found that both baseline comparisons and our methods benefit from longer training time in our implementation. Therefore, we also list 2× schedule for better comparison on the sample efficiency and quality of sample selection methods.

Results. Our method leads to significant improvements from random selection and even surpasses stratified selection given sufficient training time. Our method improves up to 8.0% (2.9%) when compared to baseline with 0.2% (1%) labeled data. In addition, CLIP selection surpasses MoCo selection in all settings, demonstrating the generality of sample selection with CLIP models that have *not* seen ImageNet in their training set. In 1% task with 2× schedule, although the difference between stratified and random sampling is only 1%, which is likely due to the limited information learned in the pretrained model, our method is able to improve 1.2% with MoCo and 1.4% with CLIP, surpassing stratified selection by 0.2% and 0.4%, respectively. This is a very promising phenomenon, since stratified sampling implicitly makes use of label information in the dataset while ours do not. In 0.2% task with 2× schedule, our method even surpasses stratified sampling by 3.8%, which shows the high quality of selected samples with our method.

A.3. Numerical Comparison with Other AL/SSAL Methods

In addition to the figure in the main text, Table 7 compares our method with other AL/SSAL methods. We have higher sample efficiency when compared to other AL/SSAL works.

A.4. Overview on Unsupervised Representation Learning

In self-supervised learning stage, we aim to learn a mapping function f such that in the $f(x)$ feature space, the positive instance x'_i is attracted to instance x_i , meanwhile, the negative instance x_j (with $j \neq i$) is repelled, and we model f by a convolutional neural network, mapping x onto a d -dimensional hypersphere with L^2 normalization. To make a fair comparison with previous arts [7], we use MoCo v2 [13] to learn representations on ImageNet with the instance-centric contrastive loss:

$$C(f_i, f_i^+, f_{\neq i}^-) = -\log \frac{\exp(\langle f_i, f_i^+ \rangle / T)}{\exp(\langle f_i, f_i^+ \rangle / T) + \sum_{j \neq i} \exp(\langle f_i, f_j^- \rangle / T)} \quad (9)$$

where T is a regulating temperature. Minimizing it can be viewed as maximizing the mutual information (MI) lower bound between the features of the same instance [32, 48]. For experiments on ImageNet, the MoCo model pre-trained for 800 epochs is used for initializing the SSL model, as in [7].

The feature spaces of CIFAR-10 data we work on are extracted with CLD [63]. The instance-group contrastive loss is added in symmetrical terms over views x_i and x'_i :

$$L(f; T_I, T_G, \lambda) = \sum_i (C(f_I(x_i), v_i, v_{\neq i}; T_I) + C(f_I(x'_i), v_i, v_{\neq i}; T_I)) + \lambda \sum_i (C(f_G(x'_i), M_{\Gamma(i)}, M_{\neq \Gamma(i)}; T_G) + C(f_G(x_i), M'_{\Gamma'(i)}, M'_{\Gamma'(i)}; T_G)) \quad (10)$$

Cross-level discrimination of Eqn. 10 (second term) can be understood as minimizing the cross entropy between hard clustering assignment based on $f_G(x_i)$ and soft assignment predicted from $f_G(x'_i)$ in a different view, where $f_G(f_I)$ is instance (group) branch, and $M_{\Gamma(i)}$ denotes the

Sample Selection	Accuracy (%)	# Initial Labels*	Label Budget
Core-Set [55] †	48.33 ± 0.49	100	150
Core-Set [55] †	50.96 ± 0.45	100	200
CBSSAL [26]	87.57 ± 0.31	100	150
DC-SSL (Ours)	91.10 ± 0.95 (↑ 3.53)	0	40
DC-SSL (Ours)	93.22 ± 0.31 (↑ 5.65)	0	100
Core-Set [55] †	53.77 ± 0.49	100	250
Core-Set + SSL [55] †	88.75 ± 0.42	100	250
CBSSAL [26]	90.23 ± 0.39	100	250
MMA [60]	91.69 ± 0.52	250	500
MMA + k-Means [60]	91.46 ± 0.38	250	500
DC-SSL (Ours)	93.63 ± 0.14 (↑ 2.17)	0	250

Table 7. Comparison with active learning methods. †: from [26]. *: We give all queries in one round and do not need initial labels. CBSSAL considers interacting with FixMatch for better performance, however DC-SSL can still *yield better performance without any initial labels*.

cluster centroid of instance x_i with a cluster id $\Gamma(i)$ [63]. Empirically, we found that CLD has great feature quality on CIFAR-10 and better respects the underlying semantic structure of data. To be consistent with original FixMatch settings, our semi-supervised learner on CIFAR-10 is trained from scratch, without using pretrained weights.

A.5. Using Euclidean Distance or Cosine Similarity?

Because the features of all instances are projected to a unit hypersphere with L2 normalization, theoretically, maximizing the cosine similarity between two nodes is equivalent to maximizing the inverse of Euclidean distance between two nodes: $\arg \max_{i,j} (\|f(x_i) - f(x_j)\|_2)^{-1} = \arg \max_{i,j} (2 - 2 \cos(f(x_i), f(x_j)))^{-1} = \arg \max_{i,j} (\cos(f(x_i), f(x_j)))$. However, empirically, using maximizing the inverse of Euclidean distance $1/d(\cdot)$ as the objective function performs better than maximizing the cosine similarity $\cos(x)$. The reason is that, when two nodes are very close to each others, $1/d(\cdot)$ is more sensitive to the change of its Euclidean distance, whereas $\cos(\cdot)$ tends to be saturated. Therefore, the function $1/d(\cdot)$ has the desired property of non-saturating and can better focus on the distance difference with closest neighbors.

A.6. General-domain Multi-modal Models

Although our method works well in both small and large scale datasets, there are still two interesting aspects that we would like to explore. First, in our approach, self-supervised models need to be re-trained for each new dataset, which is time-consuming and could potentially delay the schedule for data annotation in real-world industry. In addition, unsupervised models do not model semantic information explicitly, which may lead to confusion that could potentially be mitigated (e.g. datasets with varying intra-

class variance will take regions of different sizes and may be treated differently in an unexpected way).

To address these issues, we put our focus on a large pre-trained model that encodes semantic information. However, a large fully-annotated dataset, which is required to train a large supervised model, is very costly to obtain, and labelling the target dataset to train a supervised model defeats our purpose of requiring only a small amount of annotation on the target dataset. Fortunately, the availability of large-scale text-image pairs online makes it possible to train a large-scale model that encodes images in the general domain with semantic information. In this paper, we make use of publicly-available CLIP [50] models, a large-scale collection of models trained on Internet-crawled data with a wide general domain and use CLIP’s image model as feature extractor.

As shown in Experiments Section, using models trained on multi-modal datasets answers these two issues. Even though CLIP is never trained on our target dataset, nor does the categories in its training set match the dataset we are using, using it to select does not degrade our performance of sample selection and labeling pipeline. This indicates that the effectiveness of our label selection does not necessarily depend on whether the same pretrained model is used in the downstream task. In addition, we observe that such substitution even helps with a slightly larger annotation budget, demonstrating the effectiveness of making use of semantic information. Since we only perform inference on the CLIP model, the whole sample selection process could complete in *0.5 hours* on a commodity server using one GPU, indicating the possibility of our methods without delaying the schedule of human annotation or modifying the annotation pipeline and enables it to be used by industry on real-world dataset collection.

Note that although CLIP supports zero-shot inference by

using text input (e.g. class names) to generate weights for its classifier, it is not always possible to define a class with names or even know all the classes beforehand. Since we only make use of the image part of the CLIP model, we do not make use of prior text information (e.g. class descriptions) that are sometimes available in the real world. We leave better integration of our methods and zero-shot multimodal models to future work.

A.7. Hyperparameter Analysis

We focus on two hyperparameters in the analysis: λ , the weight for regularization, and k , the number of neighbors we use for k NN.

For hyperparam λ , we evaluated label selections with different λ values used in regularization. In this series of experiments, we select $\lambda \in \{0, 0.1, 0.5, 1.0, 3.5, 7.0\}$, where 0 indicates no regularization and larger λ indicates a stronger regularization. We then evaluate the mean accuracy from 10 runs, the standard deviation of classes, the difference with selection without regularization (i.e., $\lambda = 0$), and mean first order metric. We observe that as λ gets larger, we select more different samples compared to the case without regularization, and instance standard deviation gets lower since we are sampling more uniformly across the space. However, as a trade-off, we could not sample from area which has as high density as before because selecting samples from that area leads to selections that are close to each other, leading to a high penalty. Here, uniformity and representativeness show a trade-off and the optimal choice is to balance each other at $\lambda = 0.5$, which is demonstrated by the mean accuracy.

For hyperparam k , we find that although initially adding k contributes to a better representation estimation by considering more neighbors, adding too much to k makes the selection algorithm lose focus. We find that k around 400 is optimal for our scenario.

A.8. Run Time Discussion

CLD only takes about 4 hours to train on CIFAR-10 on a single GPU and sample selection with our method takes less than 10 minutes on CLD with one GPU. This takes significantly less GPU-time than FixMatch (120 GPU hours with 4 GPUs), which is, in turn, much less than the time for labelling the whole dataset of 50,000 samples. On ImageNet, MoCo takes about 12 days with 8 GPUs to achieve 800 epochs [33], our algorithm takes about an hour on one GPU to select samples for both 1% and 0.2% labels and in the end, FixMatch takes another 20 hours on 4 GPUs to train. Although it sounds like we are using a lot of compute time just to train a self-supervised learning model for selecting what samples to annotate, the fact is that FixMatch requires a self-supervised pretrained checkpoint to work well when the number of labeled samples is low, as demonstrated

in [7]. The only compute overhead introduced is the sample selection process, which is *negligible* when compared to the other two stages. In addition, shown in our experiments, CLIP, as a model trained on a general and diverse image-text dataset, could also be used to select samples with comparable and sometimes even better samples to label, which indicates that the self-supervised training stage is not required in our method for sample selection.

A.9. Experiment Setup for CIFAR-10

Setup for FixMatch. To maintain consistency with the original FixMatch [59], we evaluate FixMatch trained on CIFAR-10 with 2^{20} steps in total. To illustrate the ability of our algorithm to select informative samples, we evaluate both approaches on an extremely-low setting from 40 samples to 250 samples in total (4 shots to 25 shots per class on average). Since the original FixMatch is evaluated with stratified sampling on CIFAR-10, we also retrain FixMatch with random sampling with the same number of samples in total as a fair comparison. Unless otherwise stated, we train FixMatch with a learning rate of 0.03, and weight decay 10^{-3} on 4 Nvidia RTX 2080 Ti GPUs with batch size 64 for labeled samples and with 2^{20} steps in total. All experiments are conducted with the same training and evaluation recipe for fair comparisons.

Setup For Transfer-Learning Based Approach SimCLRv2-CLD. We also evaluate our algorithm on two-stage SSL method SimCLRv2-CLD based on transfer learning [12] by fine-tuning the linear layer of a ResNet-18 pretrained with self-supervised learning algorithm CLD [63]. Specifically, we fine-tune the linear layer on a ResNet-18 trained with CLD [63]. Since it is easy for the network to overfit the few-shot labeled samples, we freeze the backbone and fine-tune only the linear layer. We use SGD with learning rate 0.01, momentum 0.9, and weight decay 10^{-4} for 5 epochs because longer training time will lead to over-fitting.

Setup For MixMatch and CoMatch. For MixMatch, we train for 1024 epochs with 1024 steps per epoch, following the original recipe. For each of labeled and unlabeled dataset, we use a batch size 64. We use a learning rate 0.002 with Adam optimizer. The results are evaluated with an weighted EMA module that has decay rate 0.999 and are averaged over 20 last epochs in the test set. For CoMatch, we train for 512 epochs with official code and the default recipe.

A.10. Experiment Setup for CIFAR-10 in the Introduction Section

The setup is exactly the same as SimCLRv2-CLD used in the experiment section. We skip the 2 of 5 random seeds as explained in the experiments section. For inter-fold standard deviation, we use the first 5 selections with instances

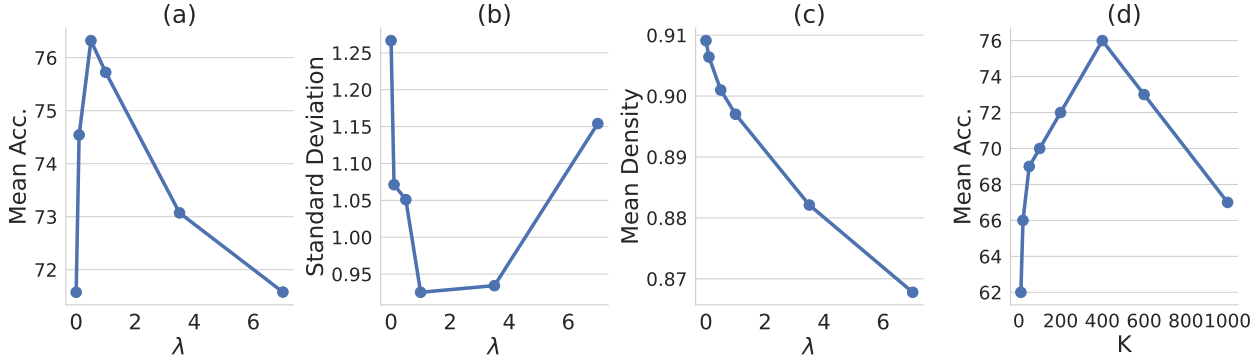


Figure 9. Effect of different hyperparameters, λ (Fig.a,b,c) and K (Fig.d). λ balances representative and uniformity across the feature space. Larger λ indicate more uniform choices but potentially less representative samples, or vice versa. Larger K indicates that we are taking more neighbors into account when estimating the representativeness, which reduces variance but may consider non-relevant samples as being represented. Due to this trade-off, considering more neighbors usually leads to better representativeness estimates, until K is greater than its optimal choice, 400.

Sample Selection	Accuracy (%) of Last Epoch / Best Epoch		
	40 labels	100 labels	250 labels
Random	82.94±9.77 / 86.67±4.71	88.72±4.61 / 91.32±2.05	93.28±0.04 / 93.69±0.05
DC-SSL (Ours)	91.10±0.95 / 91.27±0.95	93.22±0.31 / 93.55±0.33	93.63±0.14 / 93.92±0.15
Δ	↑ 8.16 / ↑ 4.60	↑ 4.50 / ↑ 2.23	↑ 0.35 / ↑ 0.23
Stratified †*	88.61±3.35	90.19±2.24	94.93 ± 0.33

Table 8. CIFAR-10 experiments with pseudo-label-based SSL method FixMatch [59], with 3 different folds, including the accuracy from last and best epoch. Fully supervised learning does not work well with such a low shot and is not reported. “Last” and “Best” indicate the accuracy of the last epoch and the best accuracy of all epochs, respectively. †: not a fair comparison with us because it assumes balanced labeled data available and leaks information about ground truth labels. Δ : gains over Random.

Sampling Method	40 Labels	100 Labels	150 Labels	250 Labels
Random	60.8 ±3.2	73.7 ±2.5	76.2 ±2.2	79.4 ±1.7
DC-SSL (Ours)	76.3 ±1.6	79.0 ±0.3	80.8 ±0.5	82.1 ±0.3
Δ	↑ 15.5	↑ 5.3	↑ 4.6	↑ 2.7
Stratified †	66.5 ±1.6	74.5 ±0.8	78.3 ±1.1	80.4 ±0.8

Table 9. CIFAR-10 experiments with transfer-learning based SSL method SimCLRv2-CLD [12, 63], with the mean and std of 5 different folds and 2 runs in each fold. †: assumes prior label information and thus not a fair comparison. Δ : gains over Random.

in all 10 classes. For intra-fold standard deviation, we select samples with the first random seed. The average accuracy for inter-fold setting is 60.67%, and the average accuracy for intra-fold setting is 60.96%. Since the inter-fold accuracy is similar to intra-fold accuracy, our selection of intra-fold setting is not biased.

A.11. Additional Experiment Results For CIFAR-10

Table 8 indicates the accuracy of last and best epochs in FixMatch experiment. We found that the accuracy from the best epoch is 3.73% higher than the accuracy from the last epoch in 40 labels task, even after taking the mean of 3 dif-

ferent folds, which indicates a phenomenon of collapsing. In comparison, our method reduces this gap to 0.17% by selecting labels that are representative and diverse.

We also present SimCLRv2-CLD with more training labels for a more comprehensive comparison in Table 9. Our improvement is prominent especially when the number of selected samples is low. In 40 (250) labels case, we are able to achieve a 15.5% (2.7%) improvement.

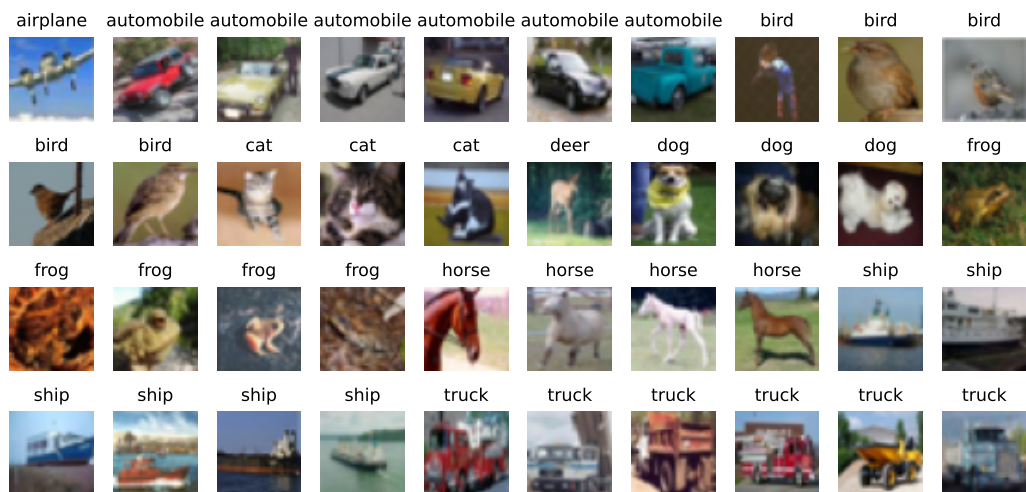
A.12. Experiment Setup for FixMatch and Supervised Learning on ImageNet

To evaluate the effectiveness of our method on large-scale datasets with more classes, we perform evaluation of

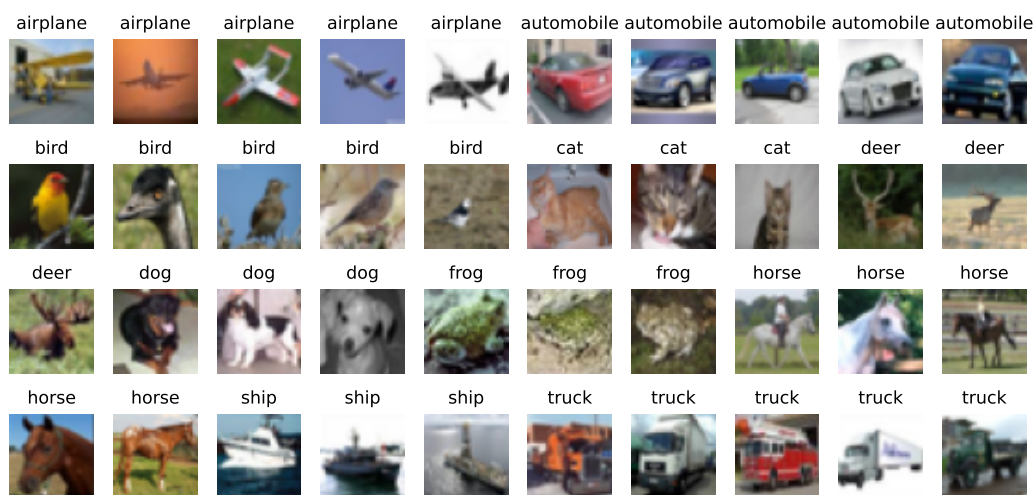
our method on ImageNet [53] with approximately 1 million images and 1000 classes. We perform supervised learning and semi-supervised learning on both 1% labeled data (12820 samples) and the extremely data-scarce setting 0.2% (2911 samples). For each of these settings, we use either a MoCo-pretrained model with Exponential Moving Average Normalization (EMAN) [7] or a CLIP ViT/16 model [21] to select samples to annotate. For ImageNet 1%, we run K -Means clustering with 12900 clusters, which is slightly more than 12820 samples we are selecting, because we observe that there will sometimes be empty clusters. For ImageNet 0.2%, we use the same number of clusters as the number of samples that we will select. In the supervised learning setting, we use a batch size of 256, learning rate 0.01, and weight decay 10^{-3} and train a ResNet-50 for 1000 epochs, with learning rate decayed by 0.1 at 700, 800, and 900 epochs. Since supervised learning only uses labeled data, training for 1000 epochs with 1% data takes about the same time to train the same network for 10 epochs with full data labeled. In the semi-supervised learning setting, we use FixMatch [59] with EMAN as our semi-supervised learning algorithm, and to maintain consistency with prior works, we use the same setting as in [7] besides the selection of input labeled data, unless otherwise stated. Specifically we use a learning rate of 0.03 with weight decay 10^{-4} and train a ResNet-50 for 50 epochs with a MoCo [33] model as pretrained model. We perform learning rate warmup for 5 epochs and decay the learning rate by 0.1 at 30 and 40 epochs. Note that we load MoCo model as the pretrained model for FixMatch for fair comparison so that the only difference between MoCo and CLIP setting is the sample selection.

A.13. CIFAR-10 Visualizations on Selected Samples

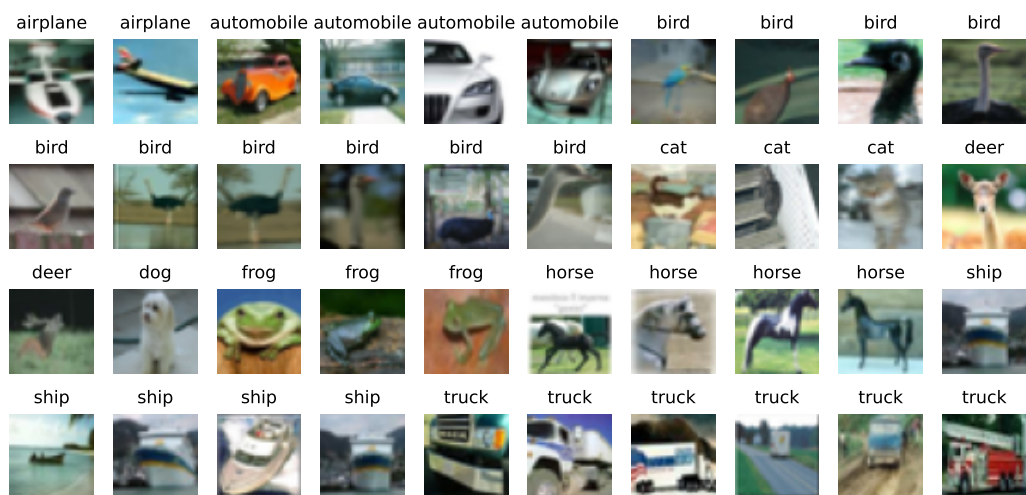
We visualize the top-40 and least-40 of our sample selection in CIFAR 10, as in Fig. 10. Random samples are highly imbalanced in terms of semantic class distribution and coverage. Our top selected samples are representative and diverse, while our least 40 selected samples are mainly outliers that could mislead the classifier.



(a) Random-40



(b) Ours: Top-40



(c) Ours: Least-40

Figure 10. Visualizations of selected samples for annotation in CIFAR-10